Geomechanics and Engineering, *Vol. 29, No. 3 (2022) 301-310*
https://doi.org/10.12989/gae.2022.29.3.301

FE model of electrical resistivity survey for mixed ground prediction ahead of a TBM tunnel face

Minkyu Kang[1a], Soojin Kim[2b], JunHo Lee[1c] and Hangseok Choi*[1]

[1]*School of Civil, Environmental and Architectural Civil Engineering, Korea University, 145 Anam-ro, Seongbuk-gu, Seoul, Republic of Korea*
[2]*Department of Micro/Nano System, Korea University, 145 Anam-ro, Seongbuk-gu, Seoul, Republic of Korea*

(Received December 27, 2021, Revised March 2, 2022, Accepted March 8, 2022)

Abstract. Accurate prediction of mixed ground conditions ahead of a tunnel face is of vital importance for safe excavation using tunnel boring machines (TBMs). Previous studies have primarily focused on electrical resistivity surveys from the ground surface for geotechnical investigation. In this study, an FE (finite element) numerical model was developed to simulate electrical resistivity surveys for the prediction of risky mixed ground conditions in front of a tunnel face. The proposed FE model is validated by comparing with the apparent electrical resistivity values obtained from the analytical solution corresponding to a vertical fault on the ground surface (i.e., a simplified model). A series of parametric studies was performed with the FE model to analyze the effect of geological and sensor geometric conditions on the electrical resistivity survey. The parametric study revealed that the interface slope between two different ground formations affects the electrical resistivity measurements during TBM excavation. In addition, a large difference in electrical resistivity between two different ground formations represented the dramatic effect of the mixed ground conditions on the electrical resistivity values. The parametric studies of the electrode array showed that the proper selection of the electrode spacing and the location of the electrode array on the tunnel face of TBM is very important. Thus, it is concluded that the developed FE numerical model can successfully predict the presence of a mixed ground zone, which enables optimal management of potential risks.

Keywords: electrical resistivity survey; mixed ground; numerical analysis; tunnel boring machine

1. Introduction

Owing to the steeply rising population density in urban areas, it is essential to develop underground structures such as traffic and utility tunnels (Broere 2016, Nam *et al.* 2020). A shield tunnel boring machine (TBM) is considered a promising method to excavate tunnels in urban areas with less noise and vibration, as well as to secure the stability of the adjacent structures (Jeong *et al*. 2018). However, during the excavation of TBM tunnels, unexpected geological risks can endanger construction safety and significantly reduce the efficiency of tunnel excavation, such as undesirable water inflow into the tunnel face and surface collapse (Chung *et al.* 2019, Kim *et al*. 2020, Bai *et al*. 2021).

Mixed ground conditions are one of the most hazardous geological risks in shield TBM tunneling (Toth *et al*. 2013). Soil-rock mixed ground conditions can cause uneven wear of cutters around rock formations, resulting in excessive cutter consumption (Park *et al.* 2018). In addition, the choice of soil conditioning methods depends on the geotechnical characteristics of excavation sites. Inappropriate additives for soil conditioning may result in a reduction in penetration rate under mixed ground conditions (Kim *et al*. 2019). Therefore, the accurate prediction of mixed ground conditions ahead of a tunnel face can minimize potential risks in advance.

However, a geotechnical investigation prior to the design stage of a tunnel primarily focuses on estimating overall geological profiles in wide areas, rendering it difficult to accurately predict the ground conditions ahead of a tunnel face. Therefore, several ground condition prediction methods that can be utilized inside the tunnel during excavation have been developed for safe tunnel excavation, such as tunnel seismic prediction (TSP), ground penetrating radar, electromagnetic exploration, and bore-tunneling electrical ahead monitoring (BEAM) (Dickmann and Sander 1996, Grodner 2001, McDowell *et al*. 2002, Kaus and Boening 2008).

In recent studies, electrical resistivity surveys have been developed for use in TBMs due to their simplicity in data processing and affordable cost (Cho *et al.* 2004, Ryu *et al.* 2008, Park *et al.* 2016, Park *et al.* 2017, Park *et al.* 2018, Lee *et al.* 2019, Lee *et al.* 2020). Furthermore, an FE (finite element) numerical model for simulating electrical resistivity surveys has been developed to estimate the effect of the electrode array and probes on the electrical resistivity (Schaffer and Mooney 2016, Mifkovic *et al.* 2021).

However, few studies on the prediction of mixed ground conditions have been conducted owing to the difficulty in simulating such conditions in front of a tunnel face.

*Corresponding author, Professor
E-mail: hchoi2@korea.ac.kr
[a]Ph.D. Candidate
[b]Ph.D. Candidate
[c]M.S. Student

ISSN: 2005-307X (Print), 2092-6219 (Online)

Therefore, in this study, an FE numerical model for simulating electrical resistivity surveys was developed to predict risky mixed ground conditions. The FE model was validated by comparing the numerical analysis results with not only the analytical solution corresponding to a vertical fault, but also the experimental results. The validated FE numerical model was applied to the tunnel excavation model, which represented the field tunneling conditions, by modifying the geometry of the FE model.

In addition, a parametric study was conducted using the tunnel excavation model to analyze the effect of geological conditions (the interface slope and the difference in electrical resistivity between two different ground formations) and the senor geometric conditions (the electrode spacing and the location of the electrode array) on electrical resistivity.

2. Background

2.1 Electrical resistivity survey

Electrical resistivity is a material property that measures the strength of resistance against electrical current flow. The electrical resistivity of the saturated ground can be varied by the electrical conductivity (inverse of electrical resistivity) of soil particles, the electrical conductivity of pore water, and the soil porosity. The electrical conductivity of a saturated ground formation (σ_{mix}) is given by Eq. (1) (Santamaria *et al*. 2001)

$$\sigma_{mix} = (1-n)\sigma_p + n\sigma_{el} + (1-n)\frac{r_p}{g}\lambda_{ddl}S_a \quad (1)$$

where σ_p is the electrical conductivity of soil particles, n is the porosity, σ_{el} is the electrical conductivity of pore water, r_p is the unit weight of soil particles, g is the gravitational acceleration, λ_{ddl} is the electrical conductivity of soil surfaces, and S_a is the specific area of soil particles. In most cases, the electrical conductivity of soil particles is relatively small compared to that of the pore water ($\sigma_p \ll \sigma_{el}$). The double-layer effect is small in sand or silt; therefore, the electrical resistivity of a saturated ground formation can be directly expressed by Eq. (2)

$$\rho_{mix} = \frac{\rho_{el}}{n} \quad (2)$$

where ρ_{mix} is the electrical resistivity of a saturated ground formation and, ρ_{el} is the electrical resistivity of pore water. As shown in Eq. (2), the electrical resistivity of a saturated ground formation is primarily affected by the pore water and the porosity of soil. In addition, the electrical resistivity of a saturated rock can be represented by Eq. (3) (Archie 1942)

$$\rho_{rock} = \rho_{el} \cdot n^{\theta} \quad (3)$$

where ρ_{rock} is the electrical resistivity of a saturated rock and θ is the shape factor that generally ranges from 1.3 to 2.5. The electrical resistivity of a saturated rock decreases as the rock has a high porosity.

The electrical resistivity can be measured using two current electrodes (A and, B) and two potential electrodes (M and, N). One current electrode supplies the current (I) and the other current electrode receives the current to form an electric potential distribution inside the ground. Next, the electrical resistivity (ρ_a) of a ground formation is computed by measuring the electric potential difference (V) between the two potential electrodes. The electrical resistivity (ρ_a) is calculated using the input current (I) and the measured electric potential difference (V), as shown in Eq. (4), (Reynolds 1997)

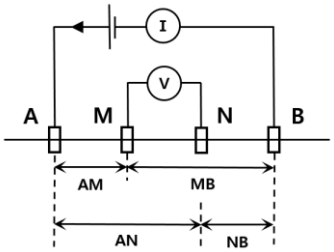

Fig. 1 Typical electrode array adopted in electrical resistivity survey

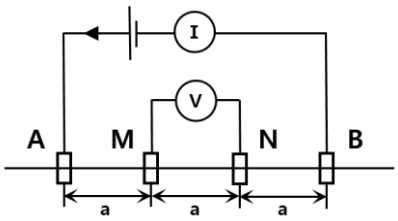

Fig. 2 Wenner electrode array configuration

$$\rho_a = 2\pi\left(\frac{1}{AM} - \frac{1}{MB} - \frac{1}{AN} + \frac{1}{NB}\right)^{-1}\frac{V}{I} \quad (4)$$

where AM is the distance between electrodes A and B, and MB, AN, and NM represent the distance between each electrode (Fig. 1).

There are several electrode array methods with distinctive characteristics such as the signal amplitude, depth of investigation, and resolution. Among the electrode array methods, the Wenner electrode array has high vertical resolution and high signal amplitude. Therefore, in this study, the Wenner electrode array was utilized to predict mixed ground conditions ahead of a tunnel. For the Wenner electrode array shown in Fig. 2, the electrical resistivity can be expressed by Eq. (5) (Telford 1990)

$$\rho = 2\pi a\left(\frac{\Delta V}{I}\right) \quad (5)$$

where ΔV is the electric potential difference between two potential electrodes M and N, I is the induced electric current between the two current electrodes, and a is the distance between the electrodes.

2.2 Analytical solution

A well-known analytical solution with the Wenner array was used to simulate electrical resistivity surveys from the ground surface. The electrical resistivity survey to predict

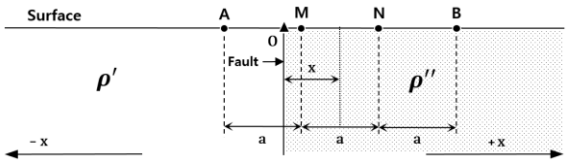

Fig. 3 Front view of the Wenner array to a vertical fault

mixed ground conditions ahead of a tunnel face is similar to an electrical resistivity survey made to detect a vertical fault from the ground surface (Fig. 3).

The apparent electrical resistivity corresponding to a vertical fault (ρ_a) from the ground surface can be represented by Eq. (6) (Van Nostrand and Cook 1966)

$$\frac{\rho_a}{\rho'} = 1 + \frac{3ka^3x}{(x^2-a^2)(4x^2-a^2)} \ , \ x < \frac{-3a}{2}$$

$$\frac{\rho_a}{\rho'} = 1 - \frac{kx(2x-3a)}{2(x-a)(2x-a)} \ , \quad \frac{-3a}{2} < x < \frac{-a}{2}$$

$$\frac{\rho_a}{\rho'} = \frac{1}{1+k}\left[1 + k^2 + \frac{ka(x+ak)}{(x^2-a^2)}\right] \ , \quad \frac{-a}{2} < x < \frac{a}{2} \qquad (6)$$

$$\frac{\rho_a}{\rho'} = \frac{1-k}{1+k}\left[1 + \frac{kx(2x+3a)}{2(x+a)(2x+a)}\right], \quad \frac{a}{2} < x < \frac{3a}{2}$$

$$\frac{\rho_a}{\rho'} = \frac{1-k}{1+k}\left[1 + \frac{3ka^3x}{(x^2-a^2)(4x^2-a^2)}\right] \ , \quad \frac{3a}{2} < x$$

where ρ' and ρ'' are the electrical resistivity values of the left and right ground formations, respectively, a is the distance between the electrodes, x is the distance from the fault to the center of the electrode array, as illustrated in Fig. 3 and k is the reflection factor expressed by Eq. (7).

$$k = \frac{\rho'' - \rho'}{\rho'' + \rho'} \qquad (7)$$

When conducting the electrical resistivity survey by shifting the electrode array, $\frac{\rho_a}{\rho'}$ in Eq. (6) should be differently expressed according to the location of the electrode array relative to the vertical fault (i.e., $x = \frac{\pm 3a}{2}, \frac{\pm a}{2}$ in Eq. (6)).

3. FE numerical solution

3.1 Verification of developed FE model

A 3D finite element model was developed using a commercial 3D FE numerical analysis program, COMSOL Multiphysics. A simplified model demonstrates the application of the numerical simulation for electrical resistivity surveys to predict mixed ground conditions ahead of a tunnel face (Fig. 4). In the numerical model, the governing equations in Eq. (8) for the electrical resistivity survey originates from the principle of Poisson's equation, which is formulated using the Gauss law and the equation of continuity as follows.

$$-\nabla \cdot (\sigma \nabla V - J^e) = Q_j \qquad (8)$$

where σ is the electrical conductivity, V is the electric

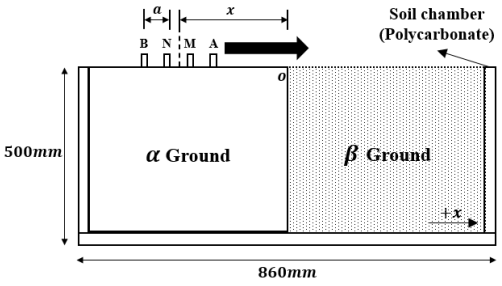

(a) Simplified model

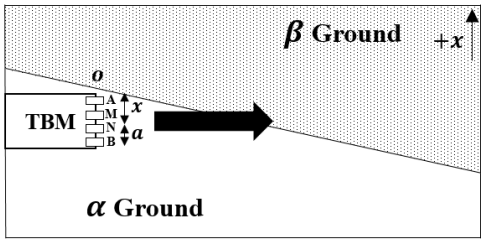

(b) Tunnel excavation model

Fig. 4 Modeling for simulating mixed ground condition ahead of a tunnel face

potential difference, J^e is the externally generated electric current, and Q_j is the current source. Next, Eq. (8) is applied to calculate the electric potential difference (V) at each node. The distribution of the current density (J) in the model was obtained from Eq. (9).

$$\vec{J} = -(\frac{1}{\rho})\vec{\nabla}V \qquad (9)$$

The electric insulation (no-flux) boundary condition was applied to the exterior boundaries of the polycarbonate soil chamber (Eq. (10))

$$n \cdot \vec{J} = 0 \qquad (10)$$

where n is a normal vector. The developed FE model was validated by comparing the numerical analysis results with laboratory experimental results as well as the analytical solution (Eq. (6)). A laboratory experiment was conducted to measure the electrical resistivity with the aid of Supersting R8 (Advanced Geosciences, Inc.) while moving the electrodes in the soil chamber (i.e., the simplified model in Fig. 4(a)). The movement of the electrodes was arranged to approximately resemble the electrical resistivity survey on a tunnel face during excavation behind mixed ground conditions, as shown in Fig. 4. The dimensions of the FE model were identical to those of the soil chamber system, as shown in Fig. 5. The material properties adopted in the numerical analysis were obtained from the measurement of the laboratory experiments and are presented in Tables 1. The granite (α ground) and gravel (β ground) were used in the laboratory experiments to simulate the mixed ground conditions. The granite and gravel were saturated with tap water for more than 24 hours.

The numerical analysis results were compared with the analytical solution for the simplified model, as shown in Fig. 6. In comparison with the analytical solution, the numerical analysis results showed a root mean square error

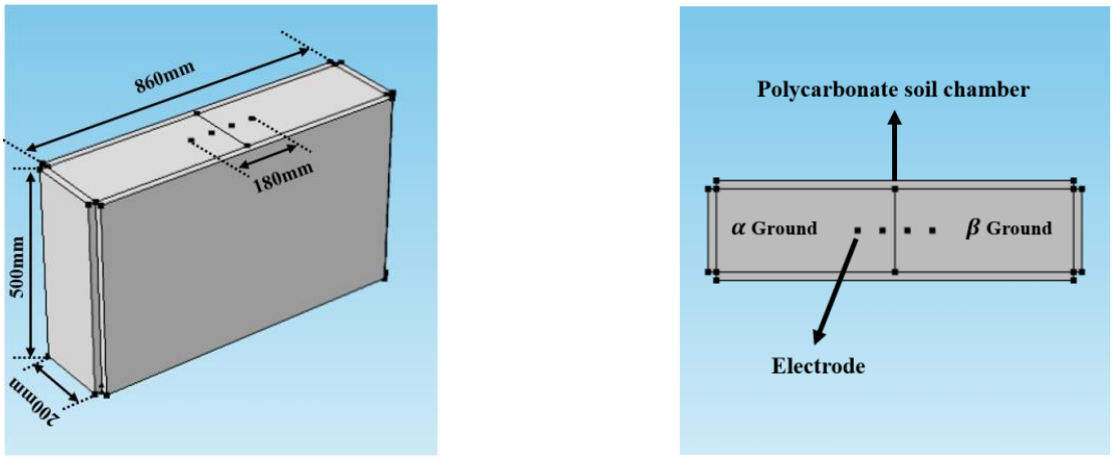

(a) Perspective view (b) Plan view

Fig. 5 FE model for simulating laboratory experiment of the resistivity survey (Simplified model)

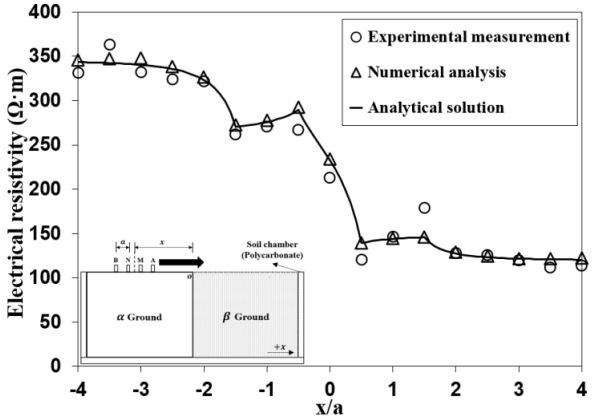

Fig. 6 Comparison of numerical analysis results with experimental results and analytical solution (Simplified model)

Table 1 Material properties adopted in FE numerical analysis and experiment

Type	Electrical resistivity ($\Omega \cdot m$)	Relative permittivity
α ground	345.7	7
β ground	119.7	20
Polycarbonate	1.15×10^{13}	0.866

(RMSE) and an average error of 2.79 $\Omega \cdot$m and 0.87%, respectively. In addition, the numerical analysis results were comparable with the laboratory experiments as also shown in Fig. 6 with a RMSE and an average error of 14.95Ω·m and 5.89%, respectively. Thus, it is concluded that the developed FE model can simulate electrical resistivity surveys with sufficient accuracy.

3.2 Effect of tunnel geometry

The verified FE numerical model was applied to the tunnel excavation model (Fig. 4(b)) to simulate electrical resistivity surveys for predicting mixed ground conditions ahead of a tunnel face. To estimate the effect of real tunnel geometry, the tunnel excavation model was compared with the simplified model. Instead of using a and x (in Figs. 4 and 6) as the variables during tunnel excavation, the tunnel diameter (D) and the distance (L) between the tunnel face and mixed ground interface were adopted as the variables, as shown in Fig. 7(a). In this study, the tunnel diameter (D) was set to 9 m, which is the typical diameter of a transportation tunnel, while maintaining the interface slopes (between two different ground formations) of 10°. The FE mesh was generated with a tetrahedral configuration. The element size selected in the FE model varied from 0.03m to 3m as shown in Fig. 7(b).

The numerical analysis results for the tunnel excavation model were compared with the analytical solution of the simplified model to estimate the effect of real tunnel geometry on electrical resistivity surveys, as shown in Fig. 8(a). The tunnel excavation model resulted in the apparent electrical resistivity values that were smaller than those in the simplified model by 21.22%. The smaller electrical resistivity in the tunnel excavation model is attributed to the boundary effect of the ground formation around the tunnel, which implies the importance of considering the tunnel geometry. However, the trends of the apparent electrical

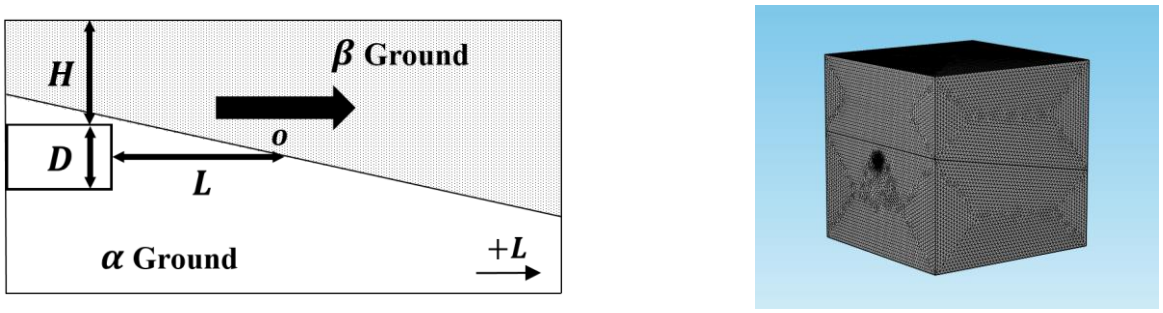

(a) Tunnel excavation model outline (b) Mesh configurations of tunnel excavation model

Fig. 7 Numerical modeling of simulating mixed ground condition ahead of a tunnel face (Tunnel excavation model)

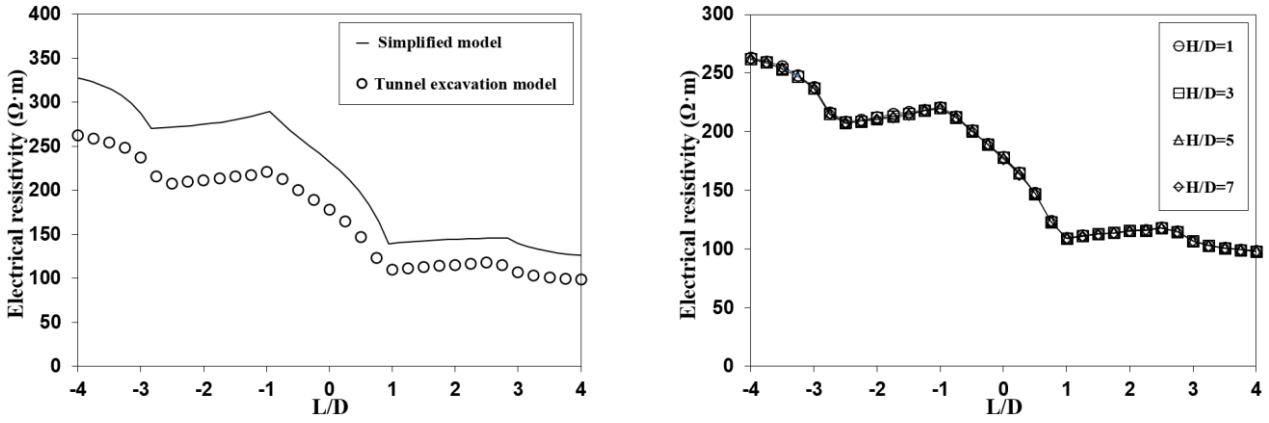

(a) Comparison of tunnel excavation model to simplified model

(b) Effect of tunnel depth (H/D)

Fig. 8 Estimation on effect of real tunnel geometry

resistivity values corresponding to L/D during tunnel excavation were similar to those of the simplified model, as shown in Fig. 8(a).

In addition, the tunnel depth (H) is practically determined according to the ground conditions around the TBM and the usage of the tunnel. Therefore, it is imperative to evaluate the effect of tunnel depth on the electrical resistivity of the tunnel excavation model. In this study, the ratio of the tunnel depth to its diameter (H/D) varies from 1 to 7, while the interface slope is maintained at 10°.

The numerical analysis results are shown in Fig. 8 (b). The tunnel depth has less impact on the apparent electrical resistivity values because the electric potential distribution around the tunnel face is mainly affected by the electric conductivity of the ground formation in front of the tunnel. As a result, the tunnel depth has little impact on the measured electrical resistivity values, and the electrical resistivity survey can be utilized to predict the mixed ground condition ahead of the tunnel face, especially in tunnels that are either too deep or shallow, which are highly susceptible to risky geological conditions.

4. Parametric study

In this study, a series of parametric studies was performed with the developed FE model (tunnel excavation model) to analyze the effect of geological conditions (i.e., interface slope and the difference in resistivity between two different ground formations) and sensor geometric conditions (i.e., electrode spacing and the location of the electrode array) on the resistivity surveys.

4.1 Effect of geological conditions

The interface slopes (θ) between the two different ground formations should be considered to simulate electrical resistivity surveys during tunneling under mixed ground conditions (refer to Fig. 9(a)). A parametric study was performed to estimate the effect of interface slopes on the electrical resistivity.

The results of the numerical analysis are compared in Fig. 9(b). As the interface slope became flatter, the electrical resistivity values followed a similar trend to the simplified model because the tunnel excavation model in this case exhibits a geometry similar to that of the simplified model.

On the other hand, the steeper slope showed a significant reduction in the electrical resistivity values when the tunnel face approached the interface, which differed from the simplified model. It is important to figure out the variation of electrical resistivity measurements corresponding to the interface slopes during electrical resistivity surveys under mixed ground conditions.

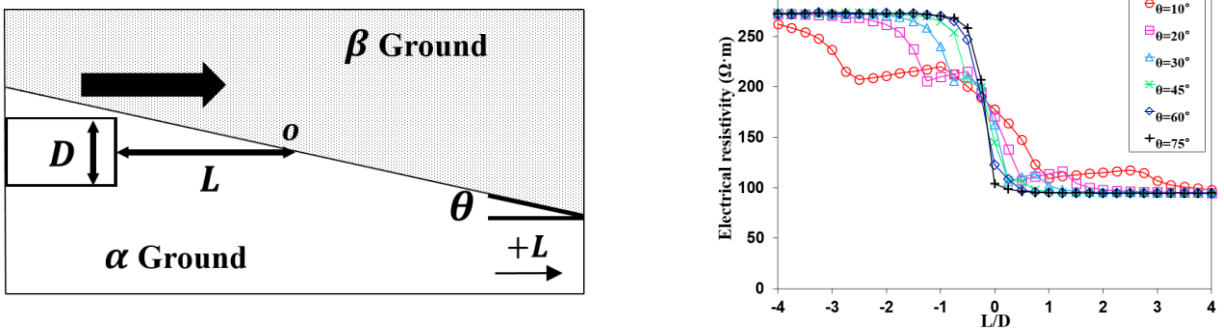

(a) Geometry of numerical model (b) Comparison of effect of interface slopes

Fig. 9 Effect of interface slopes on electrical resistivity survey

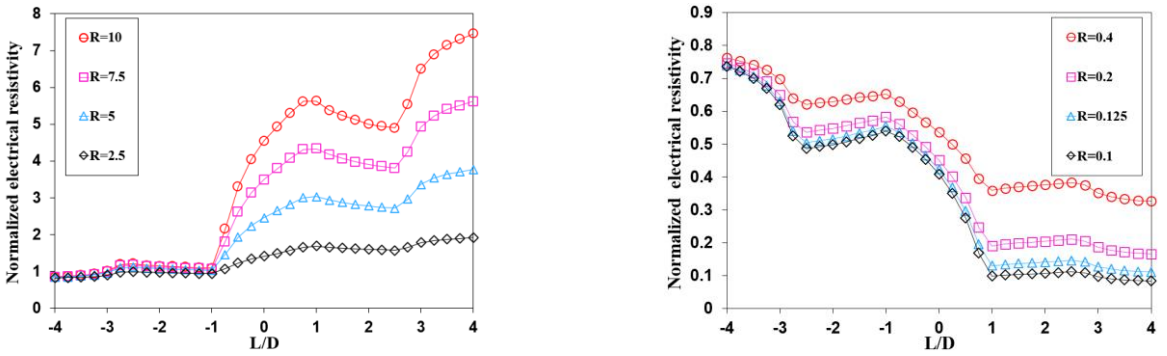

(a) Comparison of effect of R (R>1) (b) Comparison of effect of R (R<1)

Fig. 10 Effect of difference in electrical resistivity between two ground formations

The electrical resistivity implicitly indicates the ground conditions in front of a tunnel face that can affect TBM excavation (Archie 1942, Santamaria *et al.* 2001). Therefore, a parametric study was carried out to estimate the effect of the difference in electrical resistivity between two different ground formations under mixed ground conditions. The ratio of electrical resistivity of the ground formation α and β ($R = \rho_\alpha/\rho_\beta$) varies from 0.1 to 10 while maintaining the interface slopes of 10°, where ρ_α, ρ_β are the electrical resistivities of the α and β ground formation, respectively. The results of the numerical analysis are shown in Fig. 10, with a normalized electrical resistivity (ρ/ρ_α), where ρ is the measured electrical resistivity. The large difference in electrical resistivity between the two ground formations (i.e., $R = 0.1$ and $R = 10$) showed a more significant effect of the mixed ground conditions on the electrical resistivity survey. Because mixed ground conditions with large resistivity differences between two ground formations are commonly regarded as hazardous conditions, it is concluded that the electrical resistivity survey is an appropriate measure for securing safe TBM tunneling.

4.2 Effect of sensor geometric conditions

The electrode spacing (a) and the location of the electrode array (x) were usually determined according to the target ground conditions during TBM tunneling. Due to the crowded and narrow space inside an operating TBM, there are spatial restrictions on the installation of electrodes on a tunnel face. Therefore, it is vital to estimate the effect of electrode spacing and location of the electrode array on the electrical resistivity survey. In this study, the ratio of the tunnel spacing to the tunnel diameter ($3a/D$) varies from 0.4 to 1 (Fig. 11). In addition, the ratio of the distance between the center of the electrode array and tunnel invert to the tunnel diameter (x/D) varies from 0.3 to 0.7, while maintaining the electrode spacing (a) of $0.2\,D$ (i.e., $\frac{3a}{D} = 0.6$). Particularly, A parametric study for the location of the electrode array was conducted in two cases. Cases 1 and 2 represent the mixed ground conditions, where β ground is encountered at the tunnel crown and the tunnel invert, respectively, as shown in Figs. 12(a) and (b). The interface slopes (θ) between the two ground formations vary as 10°, 30°, 45°, and 75° in the numerical analysis. The electrical resistivity of the α and β ground adopted in the parametric studies is summarized in Table 1.

The numerical analysis results are shown in Figs. 13-15. As the electrode spacing increases, a reduction in the electrical resistivity occurs further ahead of the tunnel face, as shown in Fig. 13. In other words, an electrode array with a longer electrode spacing has a more extended depth of investigation. However, during overall TBM tunneling, a shorter electrode spacing represents higher electrical resistivity, which is similar to that of the simplified model.

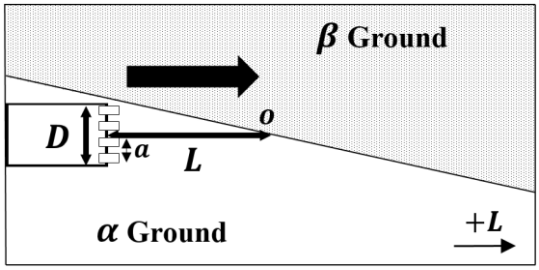

Fig. 11 Geometry of numerical model for parametric study (electrode spacing (a))

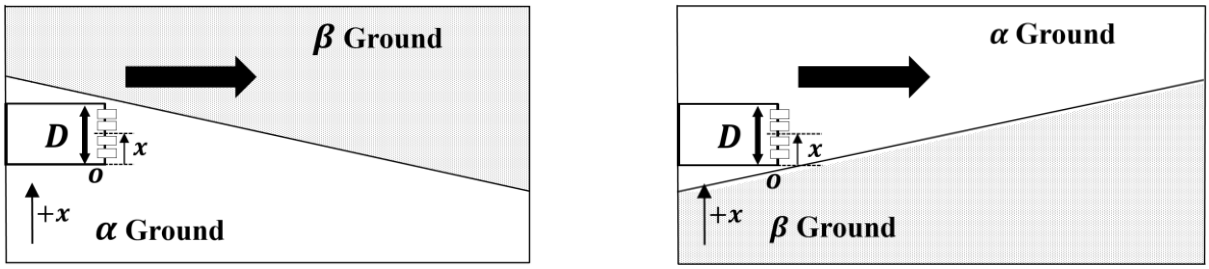

(a) Case 1 (b) Case 2

Fig. 12 Geometry of numerical model for parametric study (location of electrode array (x))

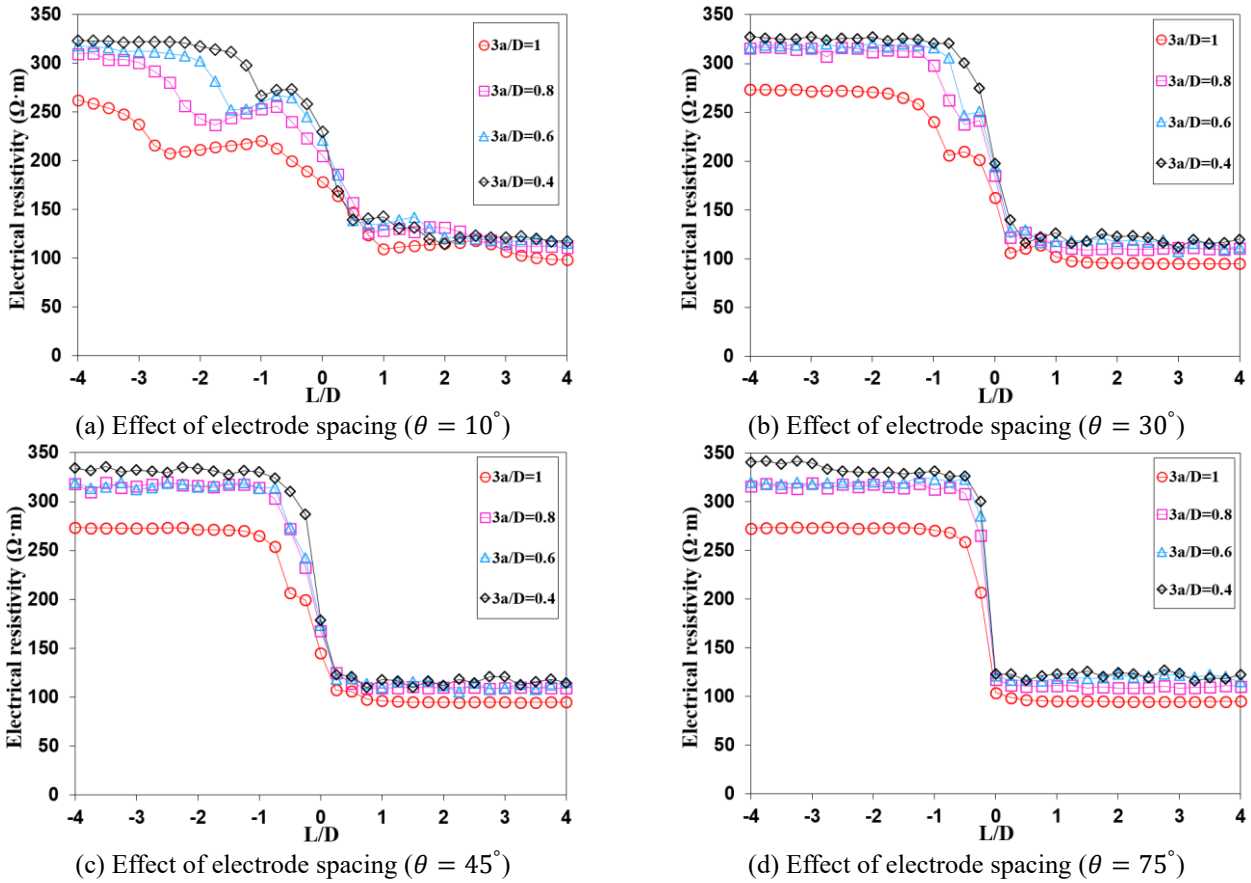

(a) Effect of electrode spacing ($\theta = 10^{\circ}$) (b) Effect of electrode spacing ($\theta = 30^{\circ}$)

(c) Effect of electrode spacing ($\theta = 45^{\circ}$) (d) Effect of electrode spacing ($\theta = 75^{\circ}$)

Fig. 13 Effect of electrode spacing on electrical resistivity survey

This trend is more evident in mixed ground conditions with lower interface slopes (that is, $\theta = 10°$). In contrast, as the interface slope became higher (that is, $\theta = 75°$), the electrical resistivity values significantly decreased when the TBM approached the mixed ground conditions, similar to that in Fig. 9(b) (Section 4.1). Thus, it is essential to predict mixed ground conditions far ahead of the tunnel face by arranging the electrode spacing in a feasible manner.

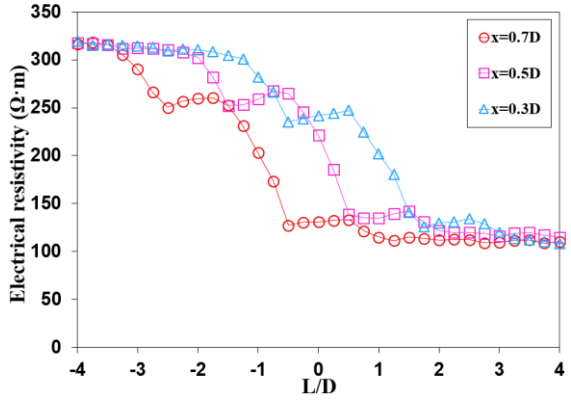

(a) Effect of location of electrode array ($\theta = 10^{\circ}$)

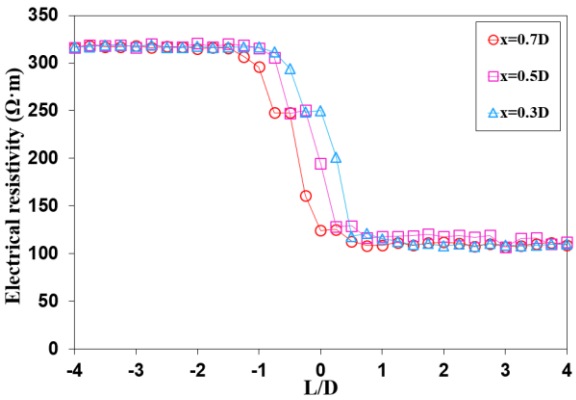

(b) Effect of location of electrode array ($\theta = 30^{\circ}$)

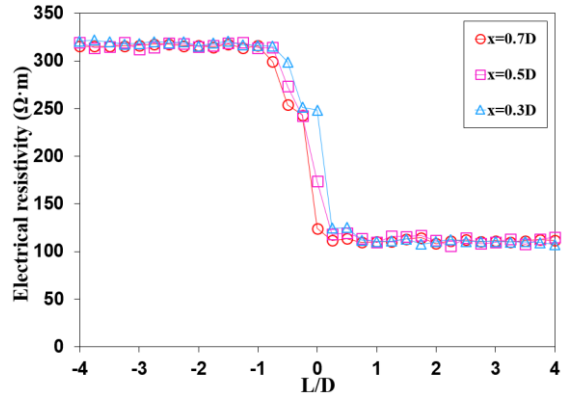

(c) Effect of location of electrode array ($\theta = 45^{\circ}$)

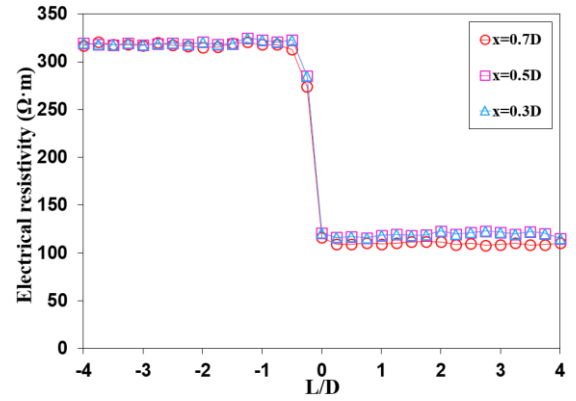

(d) Effect of location of electrode array ($\theta = 75^{\circ}$)

Fig. 14 Effect of location of electrode array on electrical resistivity survey (Case 1)

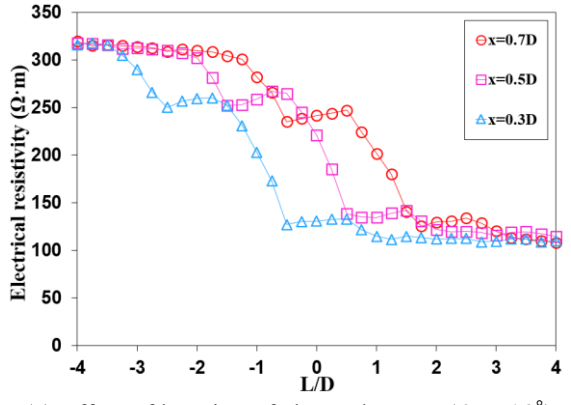

(a) Effect of location of electrode array ($\theta = 10^{\circ}$)

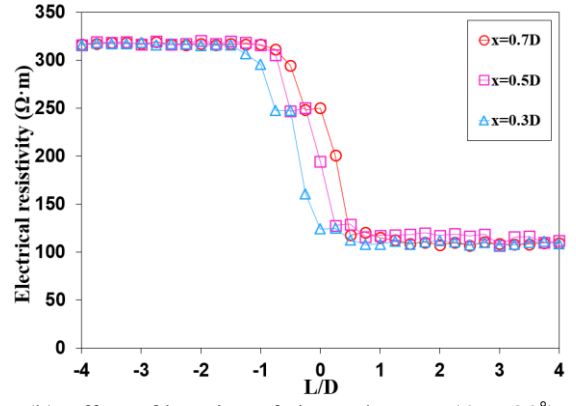

(b) Effect of location of electrode array ($\theta = 30^{\circ}$)

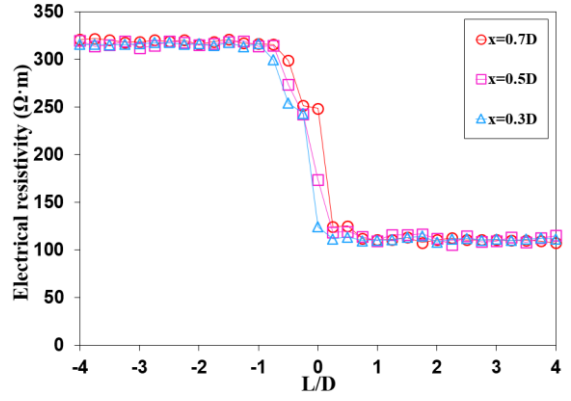

(c) Effect of location of electrode array ($\theta = 45^{\circ}$)

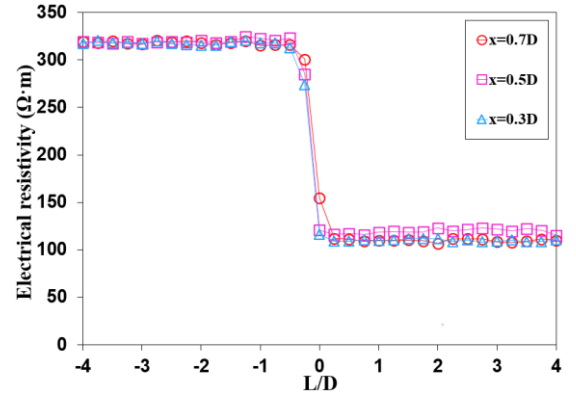

(d) Effect of location of electrode array ($\theta = 75^{\circ}$)

Fig. 15 Effect of location of electrode array on electrical resistivity survey (Case 2)

The results of the parametric study on the location of the electrode array are shown in Figs. 14 and 15. As the location of the electrode array is closer to the tunnel crown (that is, $x = 0.7D$), a decrease in the electrical resistivity arises further ahead of the tunnel face in Case 1 (Fig. 14). Conversely, when the electrode array is located around the tunnel invert (that is, $x = 0.3D$), a reduction in the electrical resistivity occurs further ahead of the tunnel face in Case 2 (Fig. 15). Similar to the effect of the electrode spacing, this trend is apparent in mixed ground conditions with a flatter interface slope. However, the steeper interface slope showed a dramatic decrease in the electrical resistivity values when the tunnel approached the mixed ground. Therefore, it is of importance to properly select the location of the electrode array on a tunnel face to perform electrical resistivity surveys under mixed ground conditions.

5. Conclusions

In this study, an FE numerical model was developed to simulate electrical resistivity surveys for the prediction of mixed ground conditions in front of a tunnel face. The FE model was validated by comparing the numerical analysis results with the electrical resistivity values obtained from the analytical solution corresponding to the simplified model, which represents a vertical fault on the ground surface. A series of parametric studies were carried out using the developed FE model to estimate the effect of geological and sensor geometric conditions on the electrical resistivity survey. The key findings and conclusions are summarized as follows.

- The effect of real tunnel geometry was examined by comparing the tunnel excavation model with the simplified model for mixed ground conditions. The tunnel excavation model resulted in smaller apparent electrical resistivity values than the simplified model by 21.22% because of the boundary effect of the ground formation around the tunnel. In addition, the tunnel depth (H) had no influence on the electrical resistivity measurements in the tunnel excavation model.
- The effect of interface slopes (θ) between two different ground formations was considered in the parametric study. As the interface slope became smaller, the electrical resistivity values followed a similar trend to the simplified model because of the similar geometry to the simplified model. However, the higher interface slopes showed a drastic reduction in the electrical resistivity values when the tunnel face approached the interface.
- The large difference in electrical resistivity between the two ground formations represents the significant effect of the mixed ground conditions, which implies that the mixed ground conditions with a large resistivity difference can be predicted using an electrical resistivity survey.
- With an increase in electrode spacing (a), a decrease in the electrical resistivity measurements occurred further ahead of the tunnel face. In contrast, the shorter electrode spacing showed a drastic reduction in the electrical resistivity values when the TBM approached the mixed ground conditions
- The location of the electrode array can affect the depth of investigation of electrical resistivity surveys depending on the geometry of the mixed ground conditions. It is essential to suitably decide the location of the electrode array on a tunnel face to promptly predict mixed ground conditions.
- The developed FE model in this study was focused on predicting only mixed ground conditions ahead of a tunnel face. Future research is needed to predict other hazardous ground conditions such as randomly scattered core stones.

Acknowledgments

This research was conducted with the support of the "National R&D Project for Smart Construction Technology (No.22SMIP-A158708-03)" funded by the Korea Agency for Infrastructure Technology Advancement under the Ministry of Land, Infrastructure and Transport, and managed by the Korea Expressway Corporation.

References

Archie, G.E. (1942), "The electrical resistivity log as an aid in determining some reservoir characteristics", *Trans. Am. Inst. Min. Metall. Eng., Society of Petroleum Engineers*, **146**(1), 54-62. https://doi.org/10.2118/942054-G.

Bai, X.D., Cheng, W.C., Ong, D.E. and Li, G. (2021), "Evaluation of geological conditions and clogging of tunneling using machine learning", *Geomech. Eng.*, **25**(1), 59-73. https://doi.org/10.12989/gae.2021.25.1.059.

Broere, W. (2016), "Urban underground space: Solving the problems of today's cities.", *Tunn. Undergr. Sp. Tech.*, **55**, 245-248. https://doi.org/10.1016/j.tust.2015.11.012.

Cho, J.S. (2004), "Rock Mass Classification and Prediction ahead of Tunnel using Electromagnetic Wave", Master. Dissertation, Korea Advance Institute of Science and Technology, Daejeon.

Chung, H. (2019), "Bayesian networks-based shield TBM risk management system: methodology development and application", *KSCE J. Civil Eng.*, **23**(1), 452-465. https://doi.org/10.1007/s12205-019-0912-6.

Dickmann, T. and Sander, B.K. (1996), "Urban underground space: Solving the problems of today's cities.", *Tunn. Undergr. Sp. Tech.*, **55**, 245-248. https://doi.org/10.1016/j.tust.2015.11.012.

Grodner, M. (2001), "Delineation of rockburst fractures with ground penetrating radar in the Witwatersrand Basin, South Africa", *Int. J. Rock Mech. Min. Sci.*, **38**(6), 885-891. https://doi.org/10.1016/s1365-1609(01)00054-5.

Jeong, H., Zhang, N. and Jeon, S. (2018), "Review of technical issues for shield TBM tunneling in difficult grounds", *Tunn. Undergr. Sp. Tech.*, **28**(1), 1-24. https://doi.org/10.7474/TUS.2018.28.1.001.

Kaus, A. and Boening, W. (2008), "BEAM–geoelectrical ahead monitoring for TBM-drives", *Geomechanik und Tunnelbau: Geomechanik und Tunnelbau*, **1**(5), 442-449. https://doi.org/10.1002/geot.200800048.

Kim, D.K., Pham, K., Park, S.Y., Oh, J.Y. and Choi, H. (2020),

"Determination of effective parameters on surface settlement during shield TBM", *Geomech. Eng.*, **21**(2), 153-164. https://doi.org/10.12989/gae.2020.21.2.153.

Kim, T.H., Kim, B.K., Lee, K.H. and Lee, I.M. (2019), "Soil conditioning of weathered granite soil used for EPB shield TBM: A laboratory scale study", *KSCE J. Civil Eng.*, **23**(4), 1829-1838. https://doi.org/10.1007/s12205-019-1484-1.

Lee, K.H., Park, J.H., Park, J., Lee, I.M. and Lee, S.W. (2019), "Electrical resistivity tomography survey for prediction of anomaly in mechanized tunneling", *Geomech. Eng.*, **19**(1), 93-104. https://doi.org/10.12989/gae.2019.19.1.093.

Lee, K.H., Park, J.H., Park, J., Lee, I.M. and Lee, S.W. (2020), "Experimental verification for prediction method of anomaly ahead of tunnel face by using electrical resistivity tomography.", *Geomech. Eng.*, **20**(6), 475-484. https://doi.org/10.12989/gae.2020.20.6.475.

McDowell, P.W., Barker, R.D., Butcher, A.P., Culshaw, M.G., Jackson, P.D., McCann, D.M., Skipp, B.O., Matthews, S.L. and Arthur, J.C.R. (2002), Geophysics in Engineering Investigations, CIRIA, London, UK.

Mifkovic, M., Swidinsky, A. and Mooney, M. (2021), "Imaging ahead of a tunnel boring machine with DC resistivity: A laboratory and numerical study", *Tunn. Undergr. Sp. Tech.*, **108**, 103703. https://doi.org/10.1016/j.tust.2020.103703.

Nam, K.M., Kim, J.J., Kwak, D.Y., Rehman, H. and Yoo, H.K. (2020), "Structure damage estimation due to excavation based on indoor model test.", *Geomech. Eng.*, **21**(2), 95-102. https://doi.org/10.12989/gae.2020.21.2.095.

Park, J., Lee, K.H., Park, J., Choi, H. and Lee, I.M. (2016), "Predicting anomalous zone ahead of tunnel face utilizing electrical resistivity: I. Algorithm and measuring system development.", *Tunn. Undergr. Sp. Tech.*, **60**, 141-150. https://doi.org/10.1016/j.tust.2016.08.007.

Park, J., Lee, K.H., Kim, B.K., Choi, H. and Lee, I.M. (2017), "Predicting anomalous zone ahead of tunnel face utilizing electrical resistivity: II. Field tests", *Tunn. Undergr. Sp. Tech.*, **68**, 1-10. https://doi.org/10.1016/j.tust.2017.05.017.

Park, J., Ryu, J., Choi, H. and Lee, I.M. (2018), "Risky ground prediction ahead of mechanized tunnel face using electrical methods: laboratory tests.", *KSCE J. Civil Eng.g*, **22**(9), 3663-3675. https://doi.org/10.1007/s12205-018-1357-z.

Reynolds, J.M. (2011), An Introduction to Applied and Environmental Geophysics, John Wiley & Sons, New York, NY, USA.

Ryu, H.H., Cho, G.C., Sim, Y.J. and Lee, I.M. (2008), "Detection of anomalies in particulate materials using electrical resistivity survey-enhanced algorithm.", *Modern Phys. Lett. B*, **22**(11), 1093-1098. https://doi.org/10.1142/S0217984908015899.

Santamarina, J.C., Klein, K.A. and Fam, M.A. (2001), Soils and Waves: Particulate Materials Behavior, Characterization and Process Monitoring", John Wiley & Sons, New York, NY, USA.

Schaeffer, K. and Mooney, M.A. (2016), "Examining the influence of TBM-ground interaction on electrical resistivity imaging ahead of the TBM", *Tunn. Undergr. Sp. Tech.*, **58**, 82-98. https://doi.org/10.1016/j.tust.2016.04.003.

Telford, W.M., Geldart, L.P. and Sheriff, R.E. (1990), Applied Geophysics, Seconded., Cambridge University Press, New York, NY, USA.

Tóth, Á., Gong, Q. and Zhao, J. (2013), "Case studies of TBM tunneling performance in rock–soil interface mixed ground", *Tunn. Undergr. Sp. Tech.*, **38**, 140-150. https://doi.org/10.1016/j.tust.2013.06.001.

Van Nostrand, R.G. and Cook, K.L. (1966), Interpretation of Resistivity Data, United States Government Printing Office, Washington, USA.